

イオンビームを用いた物性改質および分析 Ion Beam Material Modifications & Analysis

松波紀明 (N. Matsunami)

International Conference, Symposium(国際会議):

- Ion Beam Modifications of Materials (IBMM),
- Ion Beam Analysis (IBA),
- Radiation Effects in Insulators (REI) ,
- Atomic Collisions in Solids (ACS),
- Swift Heavy Ions in Matter (SHIM),
- Plasma Surface Interactions (PSI), • PFMC,
- Plasma Based Ion Implantation & Deposition (PBIID),
- Surface Modifications of Materials by Ion Beam (SMMIB),

Acknowledgements

Many staffs Nagoya University,

AIST(産総研), JAEA(原研),

NIFS (核融合研)

Many students

Outline

1. Interaction of ions with solids
2. Fundamentals of Ion Beam Analysis
3. Channeling
4. Ultra high-resolution proton energy loss spectroscopy
5. Ion beam material modification
 - (a) TiO_2 , catalysis, (b) doped-ZnO
 - (c) Reaction of N ions with nitride film
6. Plasma Surface Dynamics with IBA
in-situ D detection under plasma exposure
7. Electronic sputtering
8. Ion impact effects on graphene, Mn-doped ZnO
9. Concluding remarks

Collision of Energetic Ions with Atoms in Solids

1. Resulting in energy deposition

Elastic Collision(弹性衝突);

[atom knock-on(はじき出し)]

collisions without electronic excitation

dpa (displacement per atom) is

a measure of elastic collisions

Inelastic Collision(非弹性衝突)

electronic excitation & ionization,

usually no effects, however, in some cases
leading to atomic displacement

*イオンビームによる物性改質

1. Energy Deposition (エネルギー付与)
2. Reaction of Ions with Atoms (イオンと物質との化学反応)
3. Reaction between Ions (イオン間化学反応)

・電子・原子構造改質: Electronic & Atomic Structure Modification

・電気特性、光学特性、化学特性、磁気特性の改質

Characteristic Effects by Ion Impact?

*熱力学的非平衡: Non-thermal processing

*[損傷(damage)というイメージからの脱却]

*Ion Beam Analysis (non-destructive) イオンビーム分析 (非破壊)

組成、不純物、薄膜の厚さ (composition,
impurities, film thickness)

不純物(特に、H, C, N, O等軽元素, light
impurities)

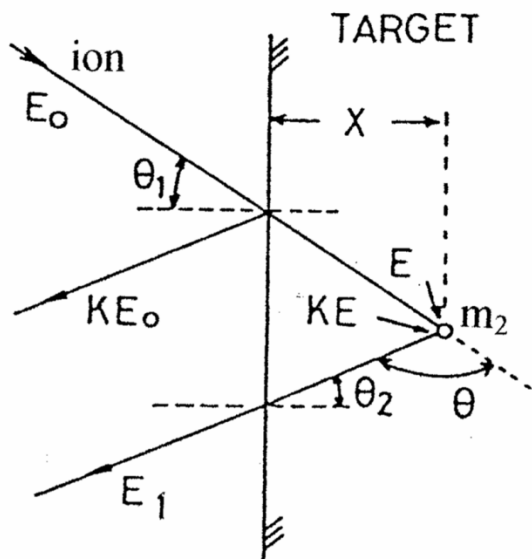
2009 brings with it the 100th anniversary of the first Rutherford Backscattering Spectroscopy experiment performed by H. Geiger and E. Marsden (a student) under the supervision of Ernest Rutherford at the University of Manchester.

Ion Beam Analysis (イオンビーム分析)

k (kinematic factor) ---> m_2 (質量)

$$\Delta E = (kE_0 - E_1) = [dE/dx] * x \rightarrow \text{depth } x \text{ (深さ)}$$

[dE/dx]: stopping power factor (阻止能因子)



$$\Delta E = k \int dx (dE/dx)_{in} / \cos \theta_1 + \\ \int dx (dE/dx)_{in} / \cos \theta_2$$

For small x (surface approximation, 表面近似),

$$[dE/dx] = \{ k(dE/dx)_{E_0} / \cos \theta_1 + \\ (dE/dx)_{kE_0} / \cos \theta_2 \}$$

RBS: Rutherford Backscattering Spectroscopy
(ラザフォード後方散乱法)

NRA: Nuclear Reaction Analysis
(核反応分析法)

ERD: Elastic Recoil Detection (弹性反跳法)

Single scattering approximation in IBA

イオン散乱分析法における 1 回弹性散乱過程

Samples (mainly Polycrystalline Thin Films)

Oxides ; ZnO, ZnO(Al, In, Mn), Cu₂O, CuO, TiO₂, SiO₂, WO₃, Fe₂O₃, SrCeO₃, High Tc superconductors etc.

Nitrides ; Si₃N₄, AlN, (TiN), Cu₃N, WN etc

Others ; C(graphite, graphene), Si, Sapphire, MgO, W, SiC

Equipments

In campus; Accelerators 2 MV AN VG,

KNVG (shut down March 2013)

200kV ion accelerator

XRD, RF-sputter film deposition

Off campus; optical, AFM(AIST)

Plasma-Material Interaction(NIFS, JAEA)

High-energy ion, RF-sputter depo.(JAEA)

Energy; ~ 200 MeV

Ion; H – Au

10 eV/u - 2 MeV/u

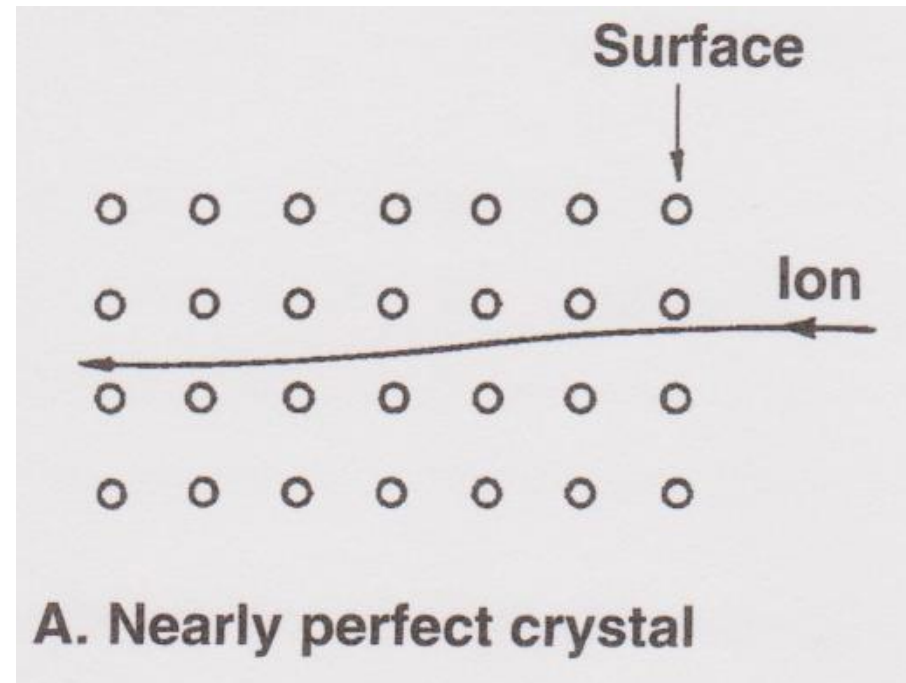
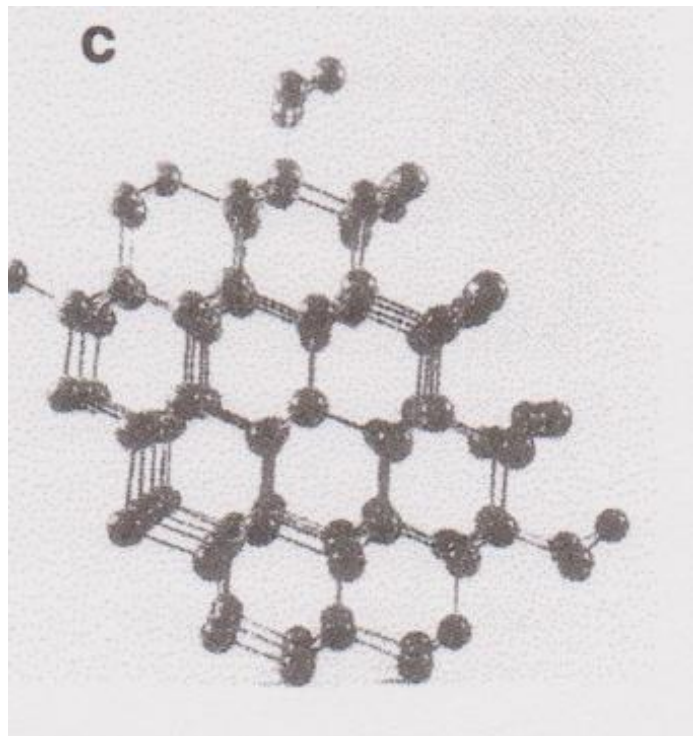
Low energy < 10 keV,

mainly elastic energy deposition

High energy >1 MeV

mainly inelastic energy deposition

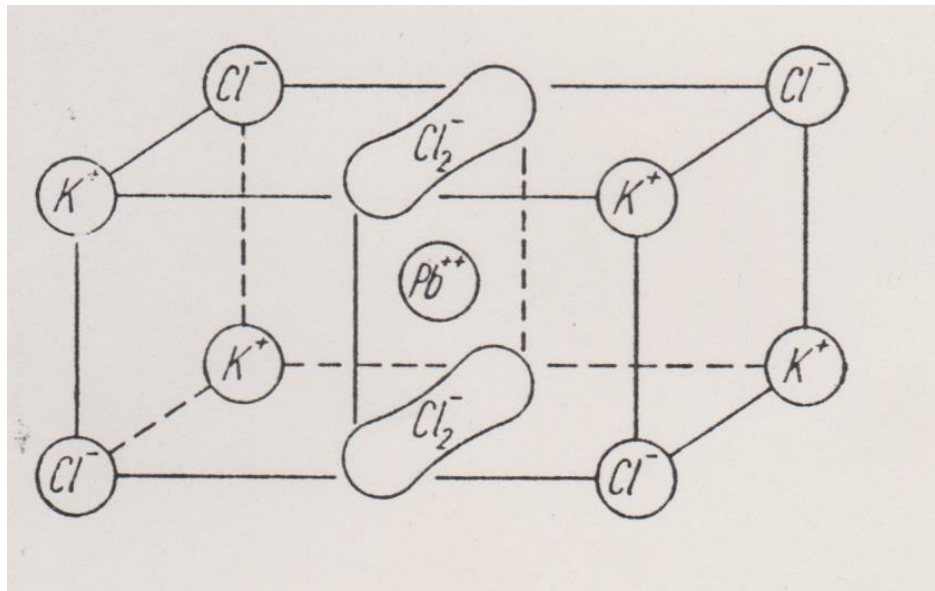
Ph. D. Thesis: Uses of Channeling Technique for Determination of Defect Concentration and Structures in Crystals (1976)



Chu, Mayer, Nicolet,
Backscattering Spectrometry,
Academic Press, 1978

Tesmer et al. ed. Handbook of modern ion beam material analysis , MRS, 1995

Location of Pb impurities in Pb-Cl interstitials in KCl



Pb is located near face center within 0.04 nm.

Matsuani, Yokoyama, Itoh, Phys. Stat. Sol. b75(1976)483.

For Al-0.1%Mn,
location of Mn
solute in Mn Al-
interstitial (mixed
dumbbell, <100>
split configuration).

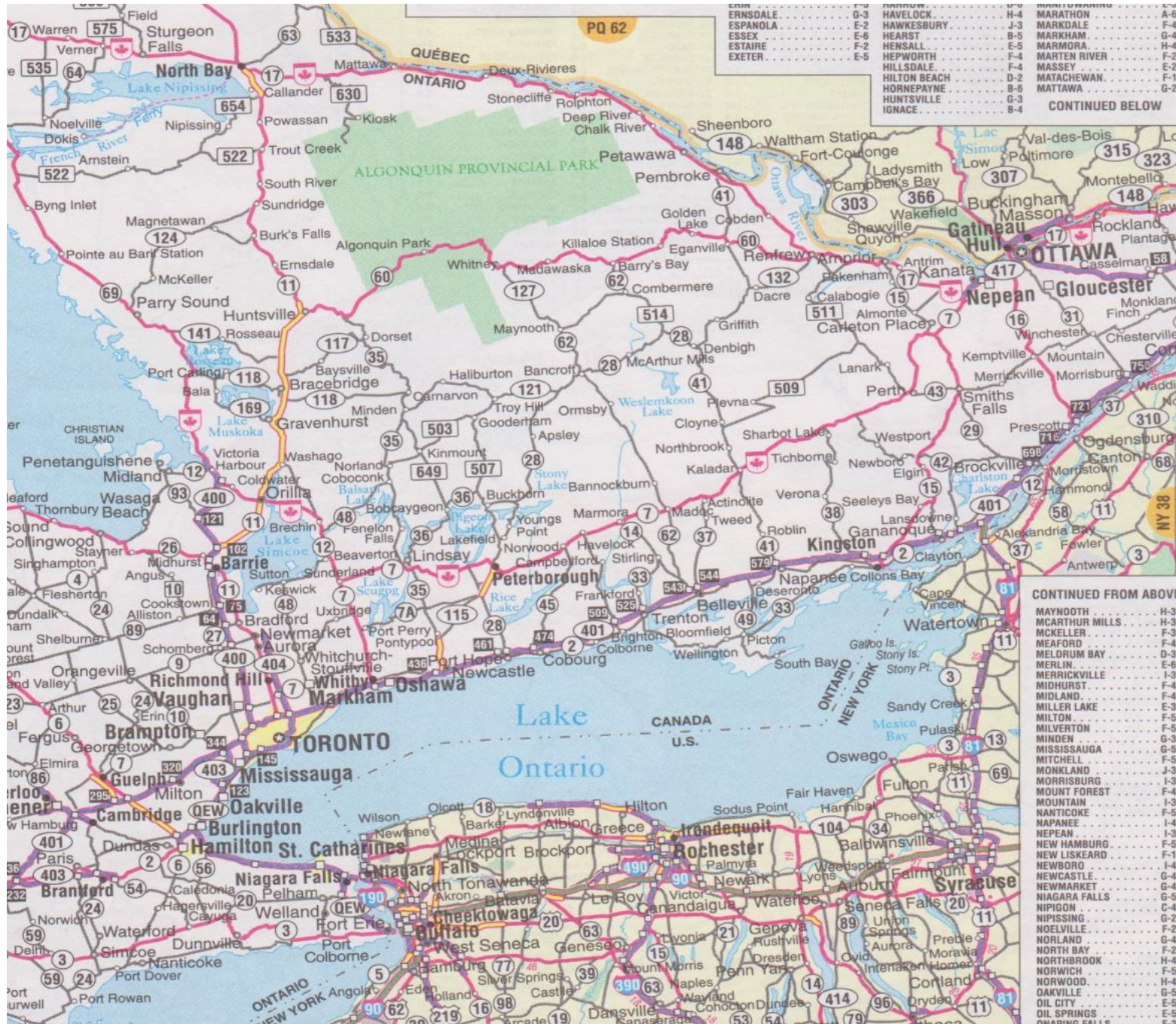
Matsuani, Swanson, Howe,
Can. J. Phys. 56(1978)1057.

1976~1978,
Solid State Science Branch, Chalk River
Nuclear Laboratories, Atomic Energy of
Canada Limited (AECL), Chalk River, Ontario,
Canada

CANADA









Mont-Tremblant Prov. Park

Surface relaxation of Pt(111)

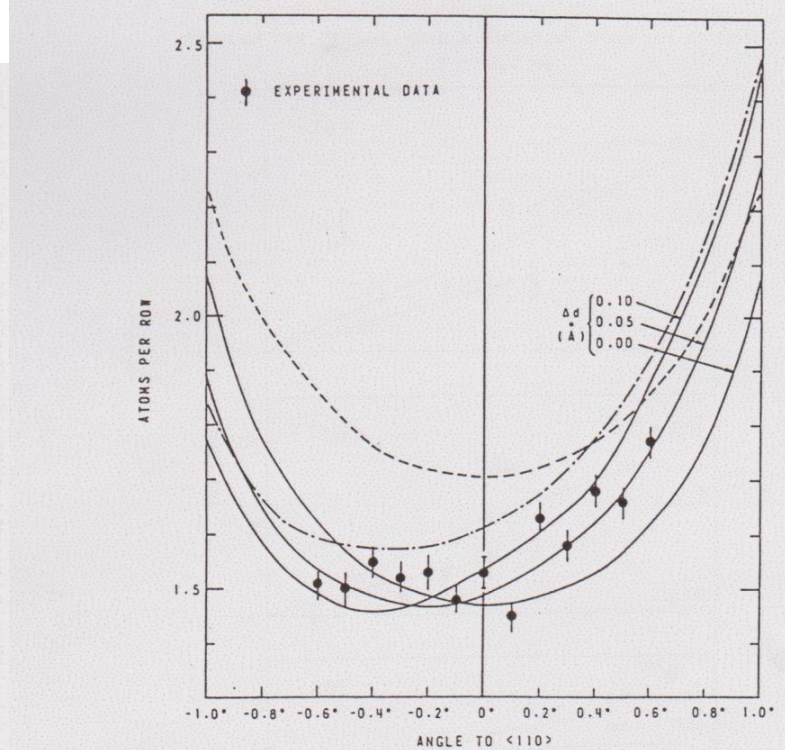
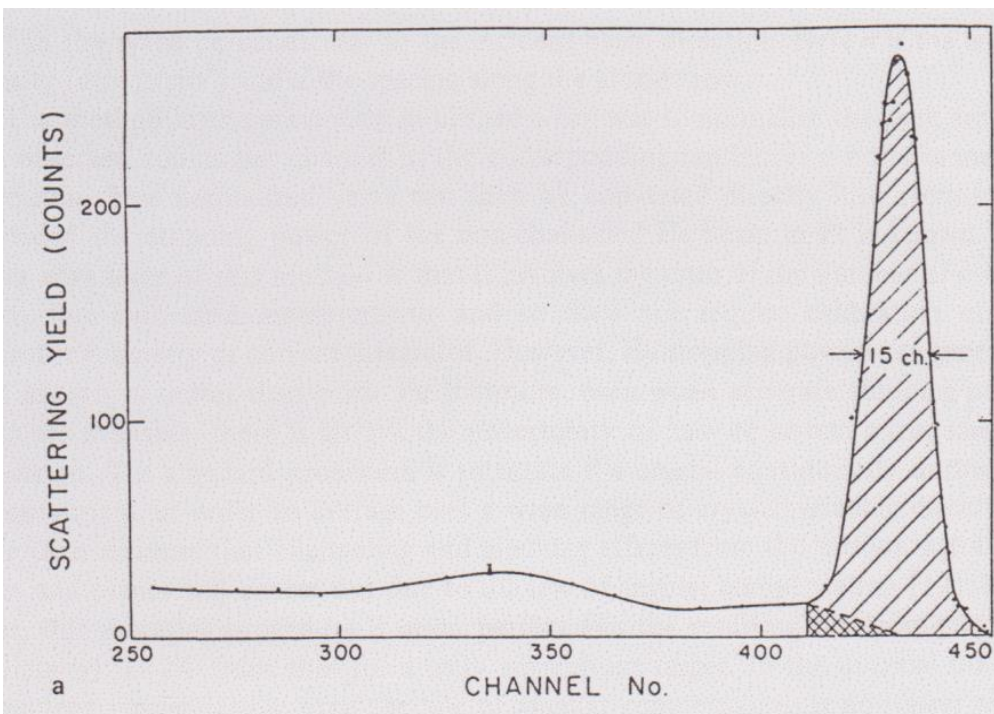


Fig. 6. Angular scan of the $\langle 110 \rangle$ surface peak on Pt(111) at 120 K using a 2.0 MeV He beam. The upper (---) curve is a Monte Carlo simulation, based on Somorjai's [21] anisotropic surface vibration value (i.e. $\theta_{\perp} = 111$ K) and assuming $\Delta d = 0$. The other curves are based on the same set of assumptions, as in fig. 5.

Outward relaxation by 0.003 nm

Davies, Jackson, Matsunami, Norton, Andersen, Surf. Sci. 78(1978)274.

Unpublished data,

Explanation is difficult to the observations.

Proton Energy Loss Spectroscopy

19

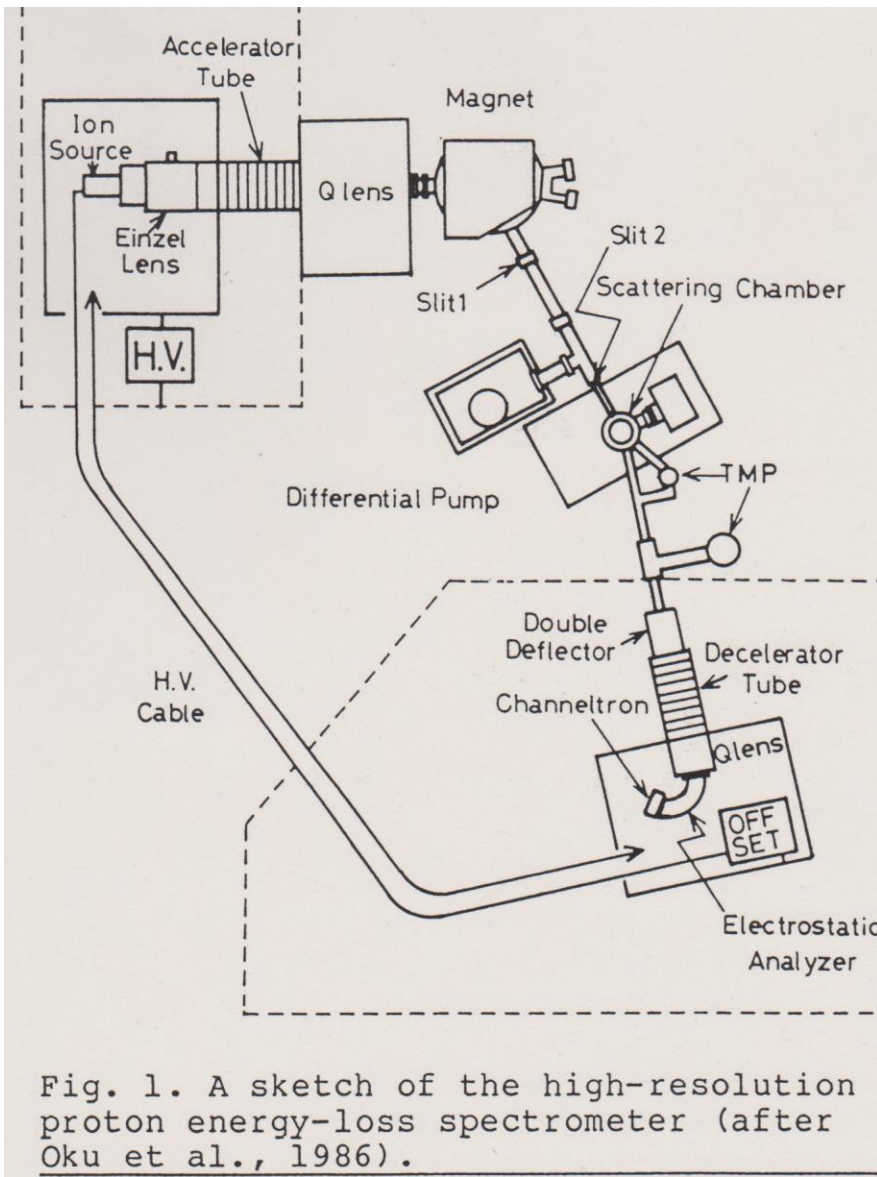


Fig. 1. A sketch of the high-resolution proton energy-loss spectrometer (after Oku et al., 1986).

100 keV Proton
Energy resolution ~20 eV,
adequate to resolve
surface monolayer.

Matsunami, Scanning
Microscopy 1(1987)1593.

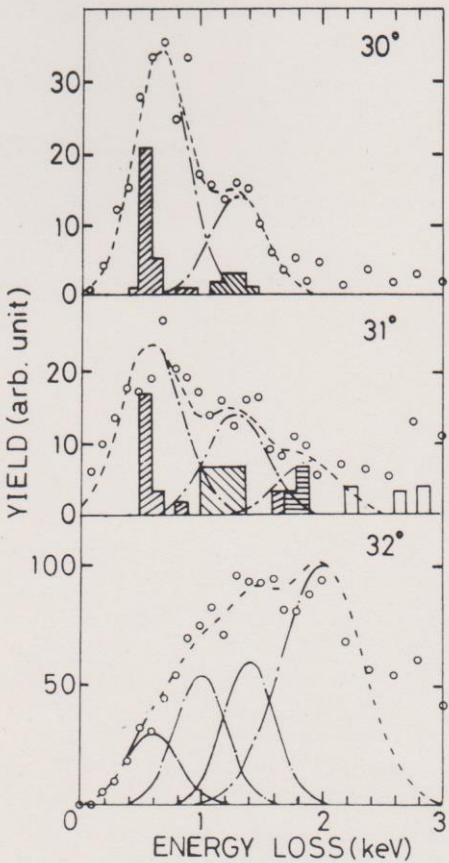


Fig. 2. Energy loss spectra of 100 keV H^+ on a W(111) surface obtained by PELS-I (open circles). Incoming and outgoing angles are 6° from the surface (scattering angle = 12°), and the azimuthal angle $\phi = 30^\circ$ means the direction along $\langle 211 \rangle$. The dashed curves are the multi-Gaussian fit to the data, and each contribution is indicated by a dot-dashed line. Histograms are the results of computer simulations for a surface contraction of ~ 5 pm and a reduced Debye temperature 200 K of the normal component of surface atom vibration. The scattering intensity from each layer is indicated by (//) for the first, (\\\) for the second, and (|||) for the third layer, respectively.

100 keV P on W(111) surface

Monolayer resolution
***Layer spacing**
Lattice vibration of
surface layer

Matsunami, Kitoh, Kanasaki, Itoh,
 NIM B45(1990)412.

Au on Si(111),
 Pd on Si(111), Pd-silicide formation

Kanasaki, Itoh, Matsunami,
 Appl. Phys. Lett. 51(1987)1072.

Energy loss in Carbon films with PELS; 100 keV Proton

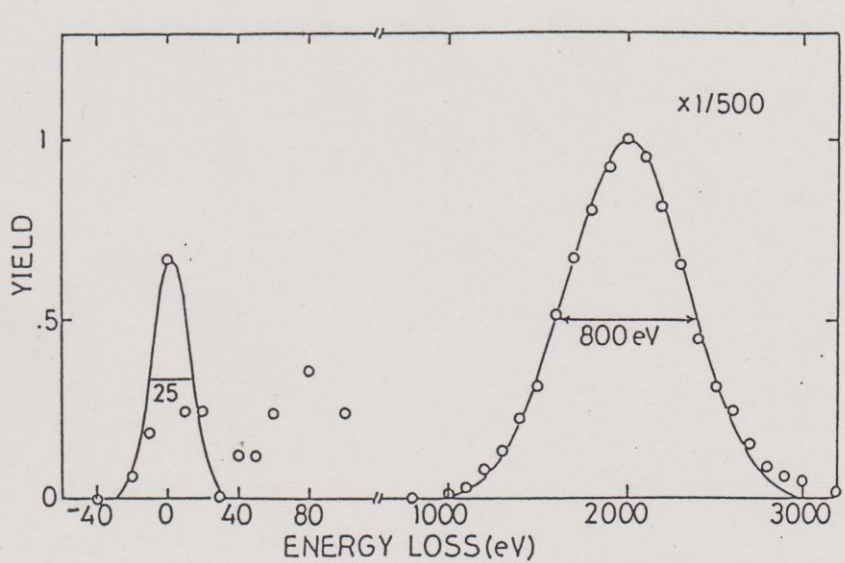


Fig.7 Energy loss spectra(ELS) for 100 keV H^+ transmitted through carbon film, showing the normal energy loss peak around 2 keV with the full width of 800 eV and the zero energy loss peak with the full width of 25 eV. Notice that the horizontal scale is different for the two peaks and $x1/500$ means that the yield of the normal energy loss peak is larger by 500 than that of the zero energy loss peak. The solid lines are the Gaussian fit.

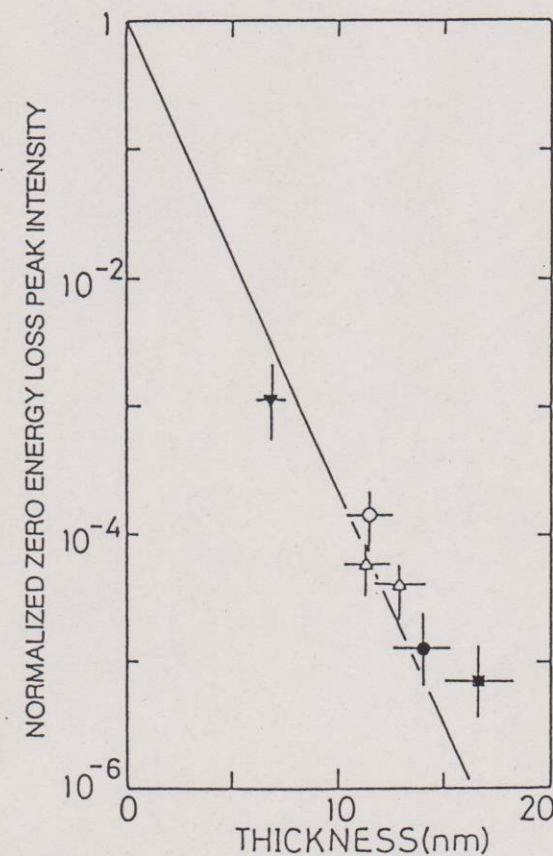


FIG.8 Normalized zero energy loss peak intensity vs thickness in nm 100 keV H^+ transmitted through carbon film. The solid line corresponds to the inelastic mean free path of 1.2 nm.

Zero energy loss;
No collisions with electrons
(no pin hole)

Matsunami, NIM B115(1999)14.
松波、科研費C(H4-5)

Inelastic mean free path (IMFP)

No collisions
with electrons

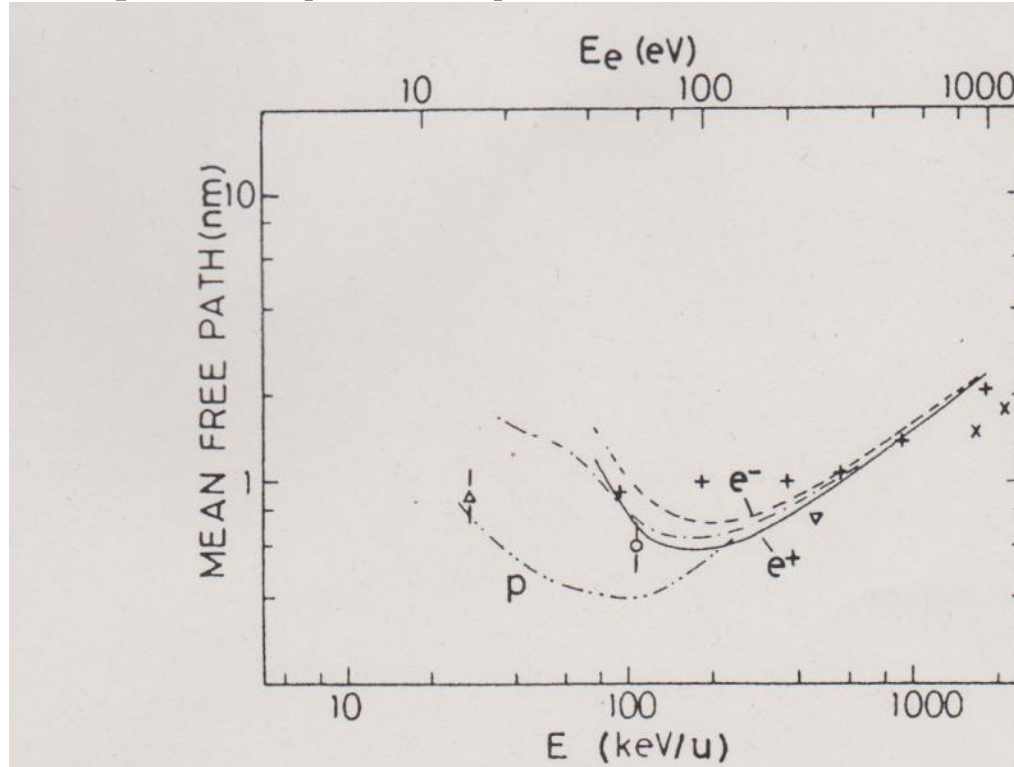


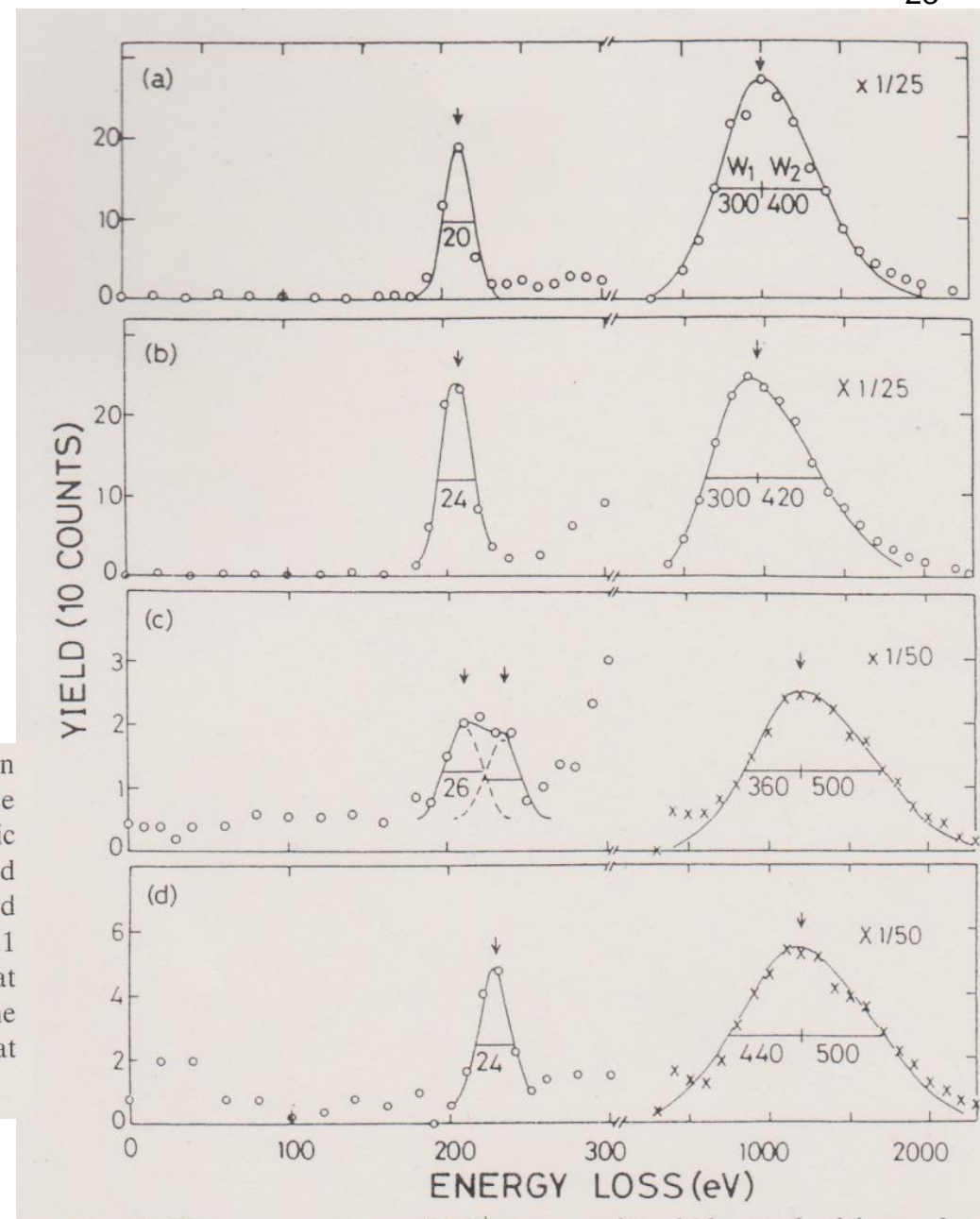
Fig. 3. Energy dependence of inelastic mean free path; present results for H^+ (\circ) and He^+ (\triangle), calculated results for positrons (solid line) and electrons (dashed line) [17]. E and E_e are the energies of H^+ , He^+ (per nucleon) and electron (or positron) having the same velocities. The dot-dashed and double dot-dashed lines show the calculated result for electrons including extension to low energies and protons, respectively, without the exchange effect after Ref. [19]. Experimental data source: ∇ = Ref. [21]; \times = Ref. [22]; $+$ = Ref. [23].

Energy loss of 100 keV Protons in C film

?Peak around 200 eV

Fig. 2. Energy spectra of H^+ transmitted through thin carbon films; (a) and (c) for 100, and (b) and (d) for 120 keV. The solid lines around the energy loss of 1 keV are the asymmetric Gaussian fit to the data. The spectra around 1 keV indicated by crosses and open circles are obtained for the as prepared sample and after bombardment of H^+ to a dose of $\sim 0.1 \mu C/mm^2$, respectively. The numbers are the half-width at half maximum in eV. The solid lines around 210 eV are the single or double Gaussian fit to the data with the full width at half maximum indicated in the figure.

Matsunami, Kitoh, NIM
B85(1985)1994)556



Ag Nano cluster formation in SiO₂-glass

150 keV Ag ion into SiO₂-glass

Interactions
between
implanted Ag's

Matsunami, Hosono,
Appl. Phys. Lett. 63
(1993)2050.

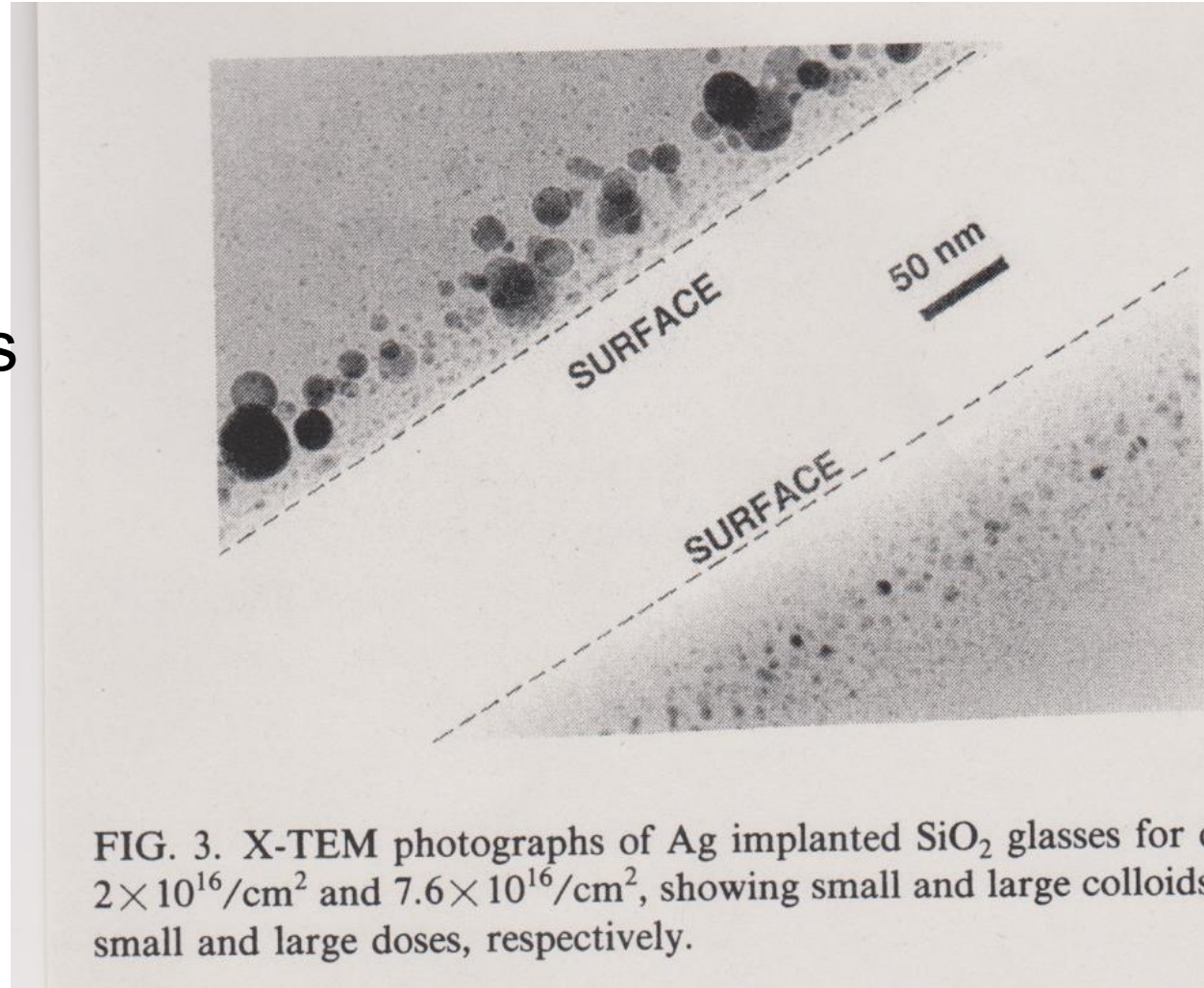


FIG. 3. X-TEM photographs of Ag implanted SiO_2 glasses for doses $2 \times 10^{16}/\text{cm}^2$ and $7.6 \times 10^{16}/\text{cm}^2$, showing small and large colloids for the small and large doses, respectively.

RESISTIVITY MODIFICATION of High T_c Cu oxide superconductors by ion impact

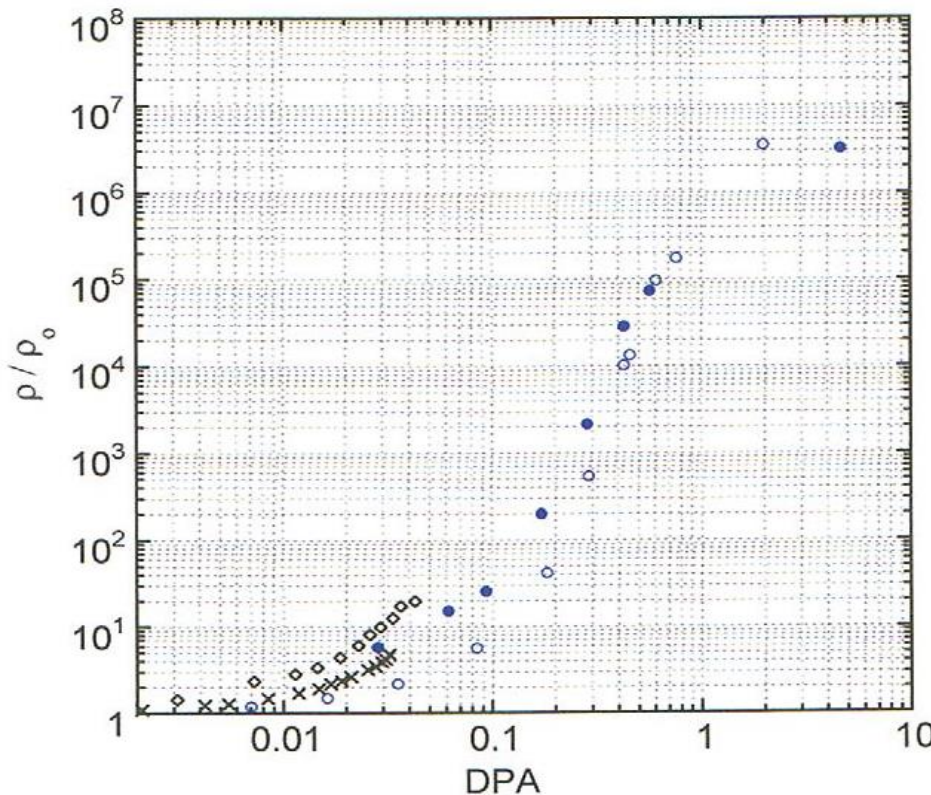
PRDPAYBCOK2a
2000.10.2

YBCO

ρ / ρ_0 vs DPA

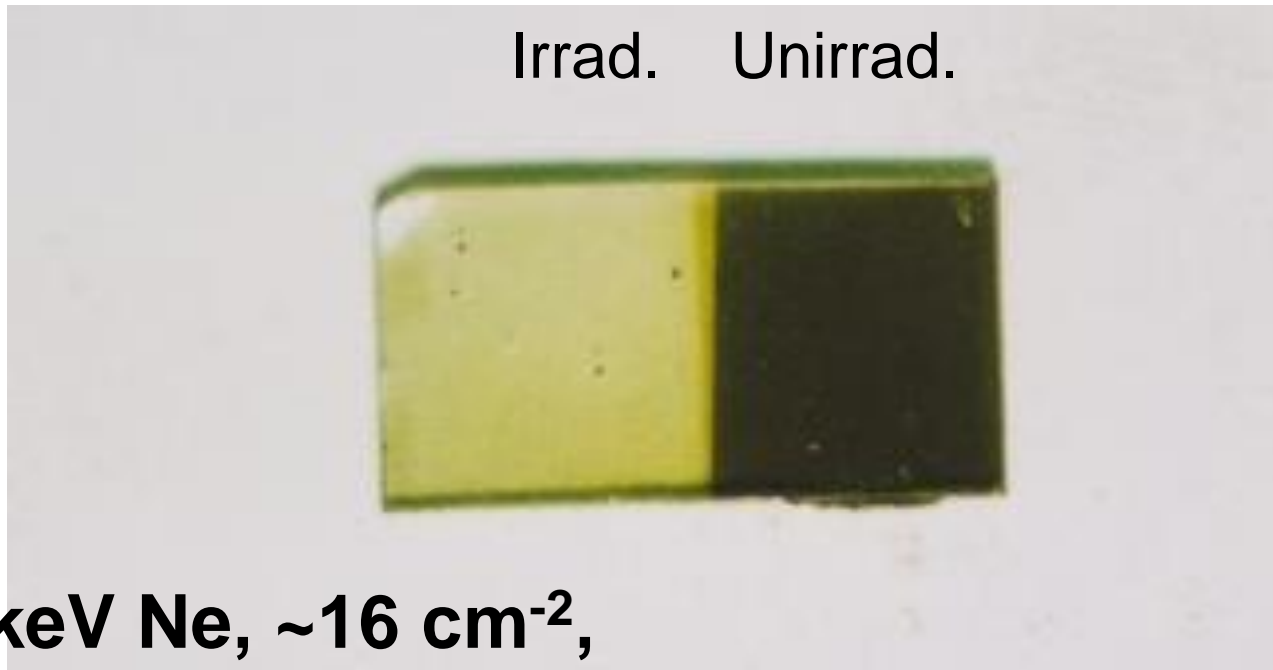
- 120 keV He
- 120 keV Ne
- × 300 keV H
- ◊ 600 keV Ar

	ρ_0 (mΩcm)	d(nm)	DPA($10^{15}/\text{cm}^2$)
	0.61	134	0.0122
	0.85	90	0.727
	(0.14	150)	0.000423
			1.04



unpublished

Low energy ion irradiation effects on HTc superconductor (YBaCuO-1237, BiSrCaCuO-222310)



unpublished

5 keV Ne, $\sim 16 \text{ cm}^{-2}$,

Projected range $\sim 7 \text{ nm} << \text{film thickness } \sim 100 \text{ nm}$
How ion irradiation effects beyond the projected range?

Low energy ions (<10 eV) in solids ?

略歴	松波紀明 2013.3.6
1967(S42)	名古屋大学工学部原子核工学科入学
1971(S46)	同上卒業
1971(S46)	名古屋大学大学院工学研究科原子核専攻入学
1976(S51)	同上終了、工学博士 学位論文: Uses of channeling technique for determination of defect concentration and structures in crystals
1976(S51)	名古屋大学工学助手
1976~1978	Solid State Branch, Chalk River Nuclear Laboratory, Atomic Energy Canada Limited (AECL)
1986(S61)	名古屋大学工学講師
1992(H4)	名古屋大学工学助教授
2003(H15)	名古屋大学理工総研助教授
2005(H17)~	名古屋大学エコトピア科学研究所准教授

共同研究(学外)等

産総研(2002 ~)

核融合科学研究所(1980頃~)

原研東海(1999 ~)

* 产学連携重点研究(2007~)(代表:2007~2012)

「高速重イオンによる電子励起効果と物性改質」

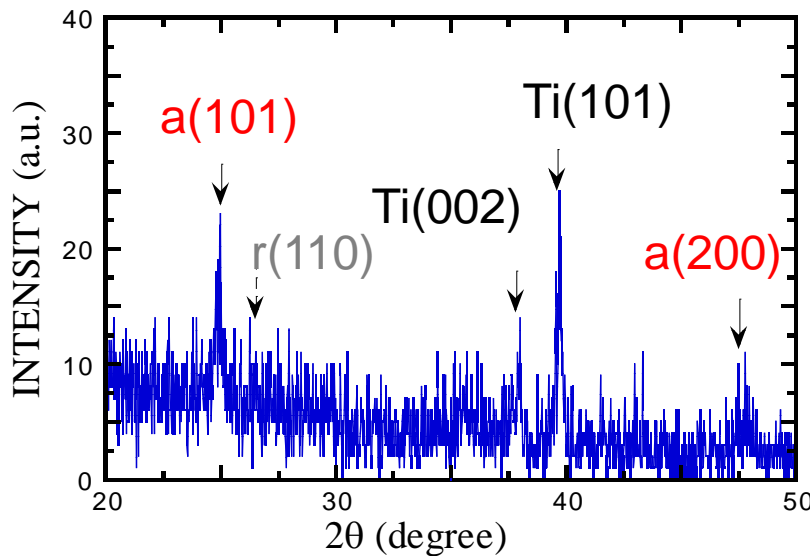
* プラズマ壁相互作用に関する調査:

炭素材の化学スパッタリング(2007~2010)

Ion irradiation effects on catalytic activity of TiO₂

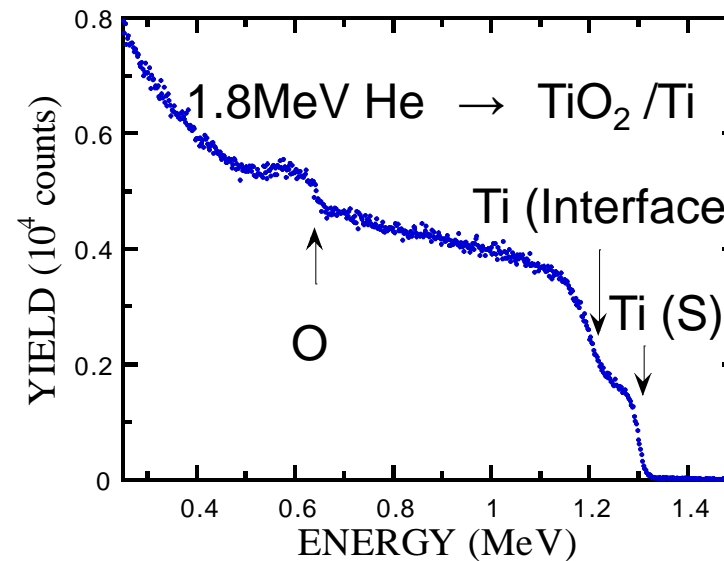
TiO₂ Film Characterization

X-ray diffraction



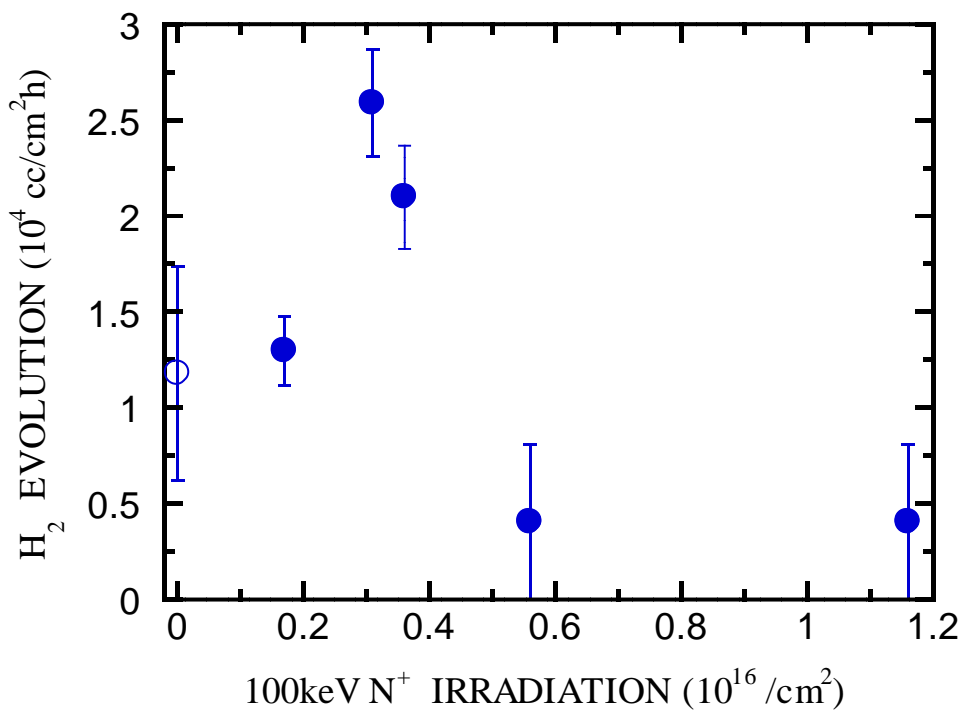
Structure
a: Anatase,
r: Rutile was not observed.

Rutherford backscattering spectroscopy (RBS)



Thickness 120 nm
Composition O/Ti=2.0±0.1

Enhancement of photocatalytic activity of anatase-TiO₂ by N ion irradiation



H_2 evolution vs N ion fluence

100 keV N ion
irradiation =>
enhancement by 2

Factors of enhancement

- Valency modification
($Ti^{+4} \rightarrow Ti^{+3}$)

- Problems
 - Area modification ?
 - Carbon contamination

Similar enhancement (a factor of 1.5) was observed for Ni-loaded Rutile- TiO_2

Optimization of Ni concentration by N ion irradiation

Dopant replacement by ion impact: In-doped ZnO

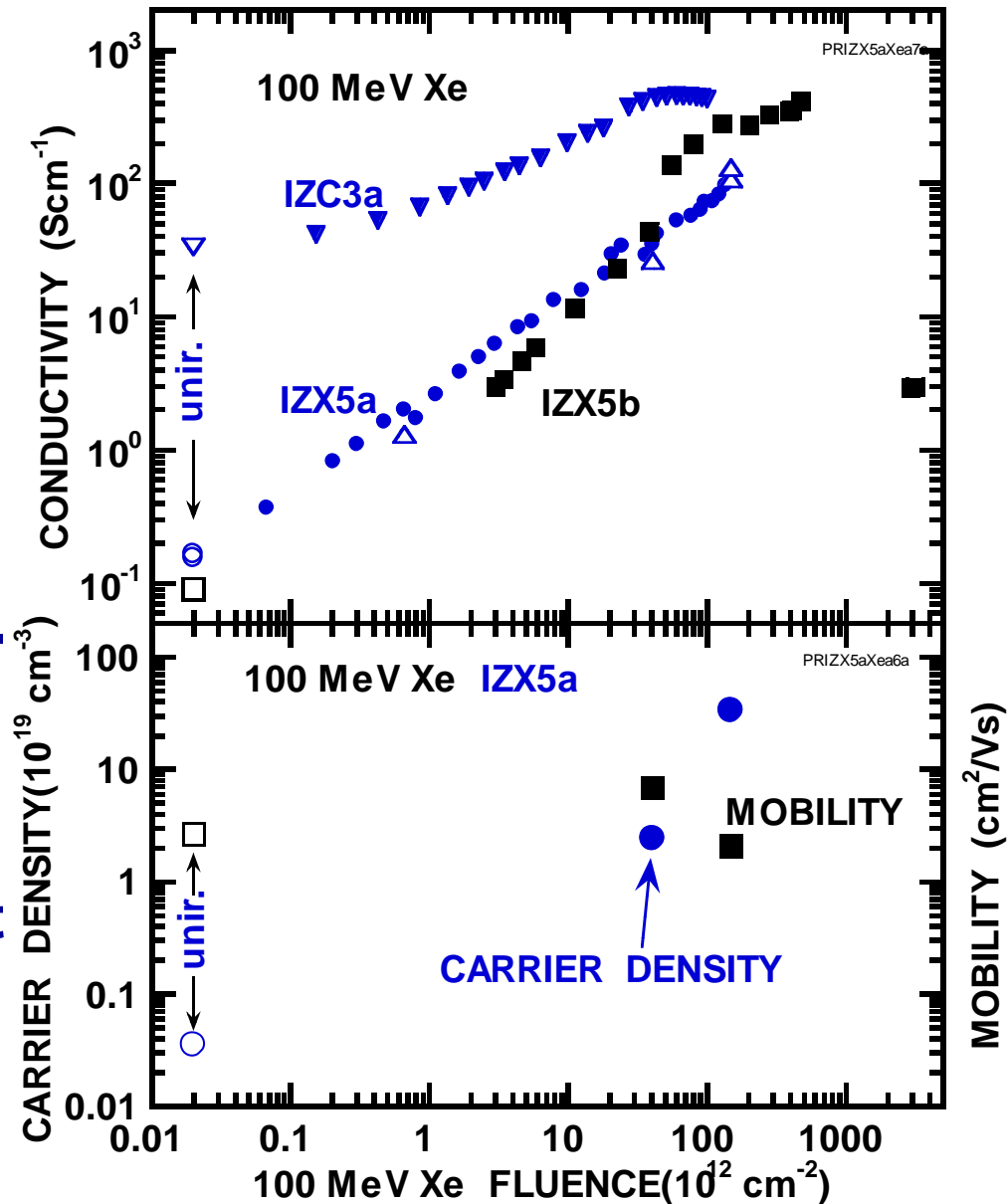
6% In doped ZnO
Unirrad. : 5~0.03 Ohmcm

- Conductivity: increase by 4 order of magnitude
 - Main factor is the carrier (electron) conc. increase due to **dopant replacement.**
- In into Zn sites

Non-thermal effect

- Direct evidence of dopant replacement?**

Matsunami, Fukushima, Sataka,
Okayasu, Kakiuchida, NIM
B268(2010)3071.



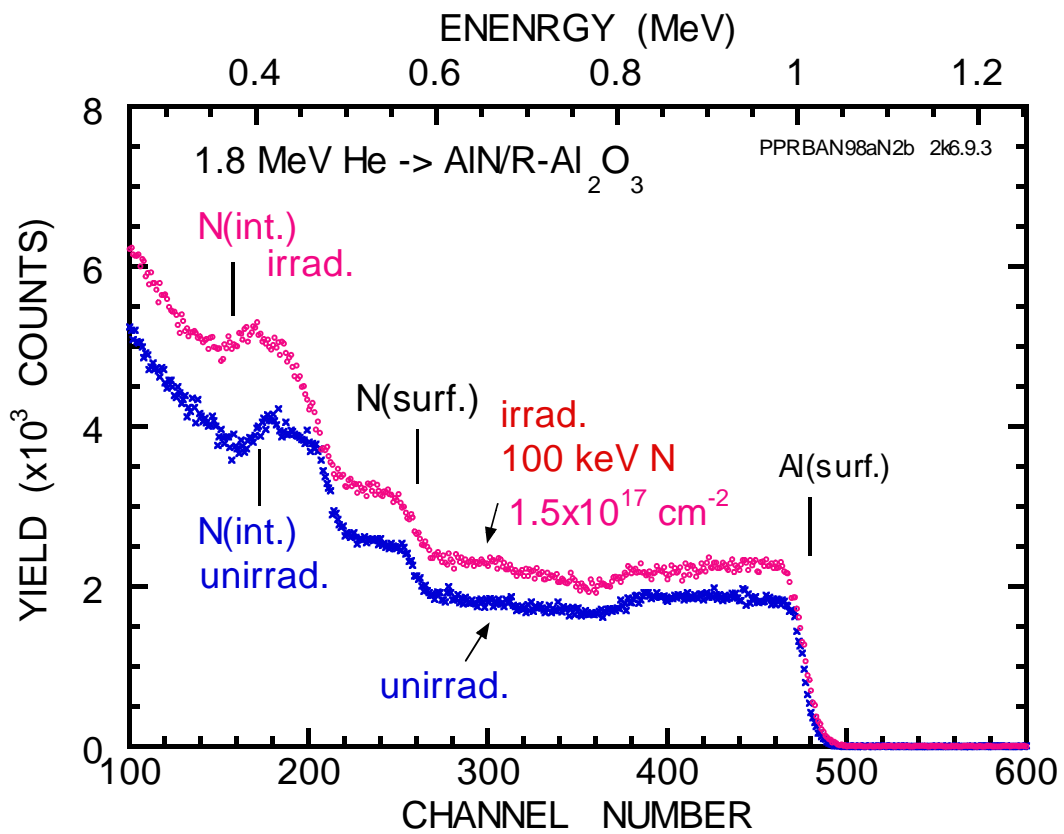
Similarly dopant-replacement induced by ion impact, i.e., conductivity increase was observed for Al-doped ZnO, Mn-doped ZnO.

***Direct evidence of dopant-displacement by ion impact**

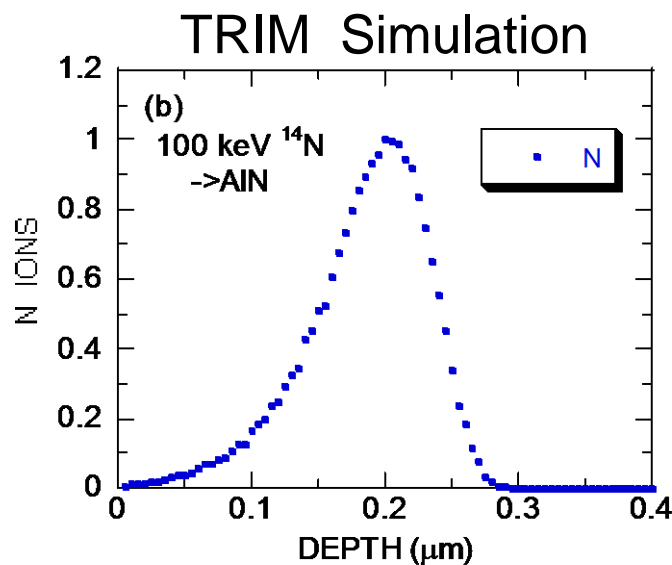
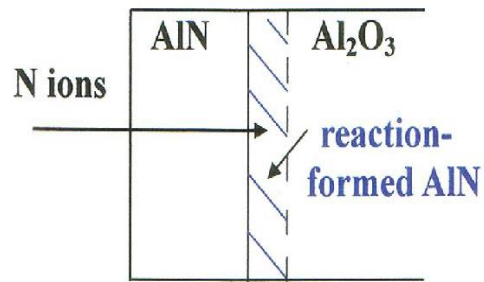
XEAFS

Reaction of N ions with nitride films near film to substrate interface (Interface reaction)

Interface reaction: non-thermal (AlN/Al₂O₃)

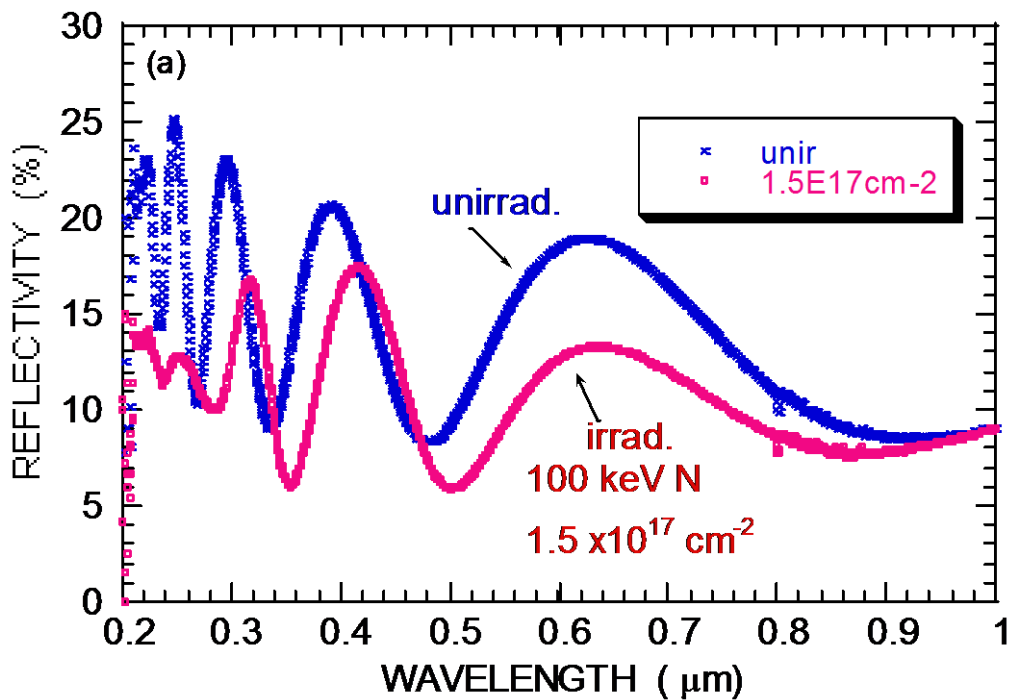


Interface reaction was also observed for Si_3N_4 (amorphous, $\sim 0.2 \mu\text{m}$) / SiO_2 .



- Increase of film thickness by 100 keV N ion irradiation
- Optical reflectivity also shows film thickness increase
- N-Al(Al_2O_3) reaction, growth of AlN layer

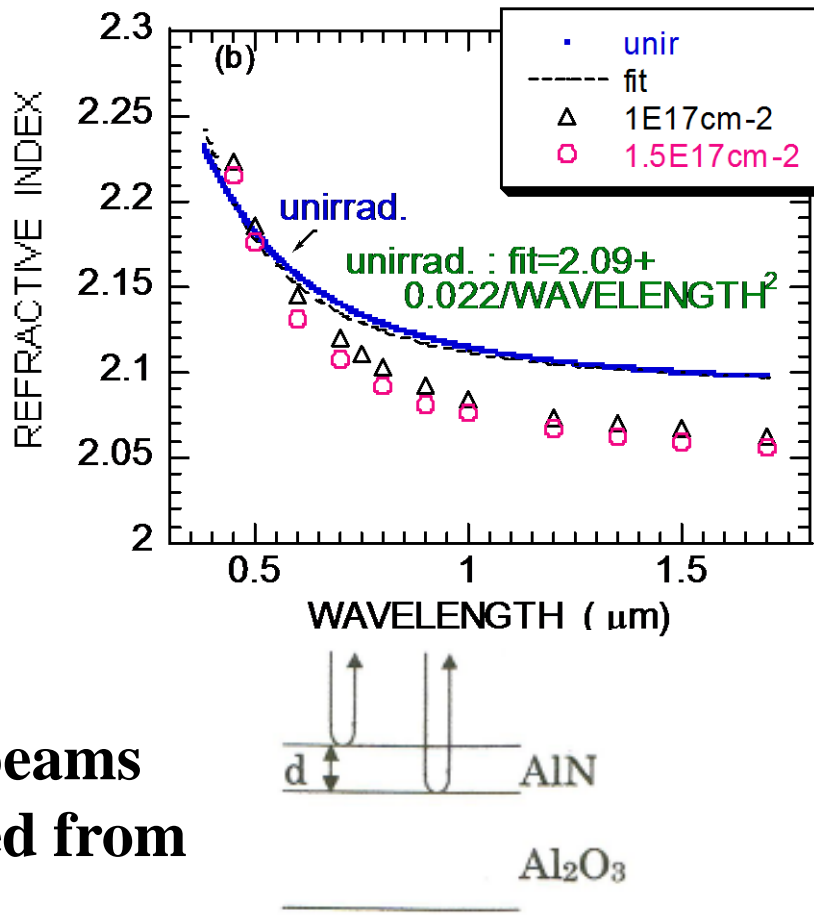
Optical reflectivity



Oscillations: Interference of photon beams between directly reflected and reflected from AlN-Al₂O₃ well-defined interface

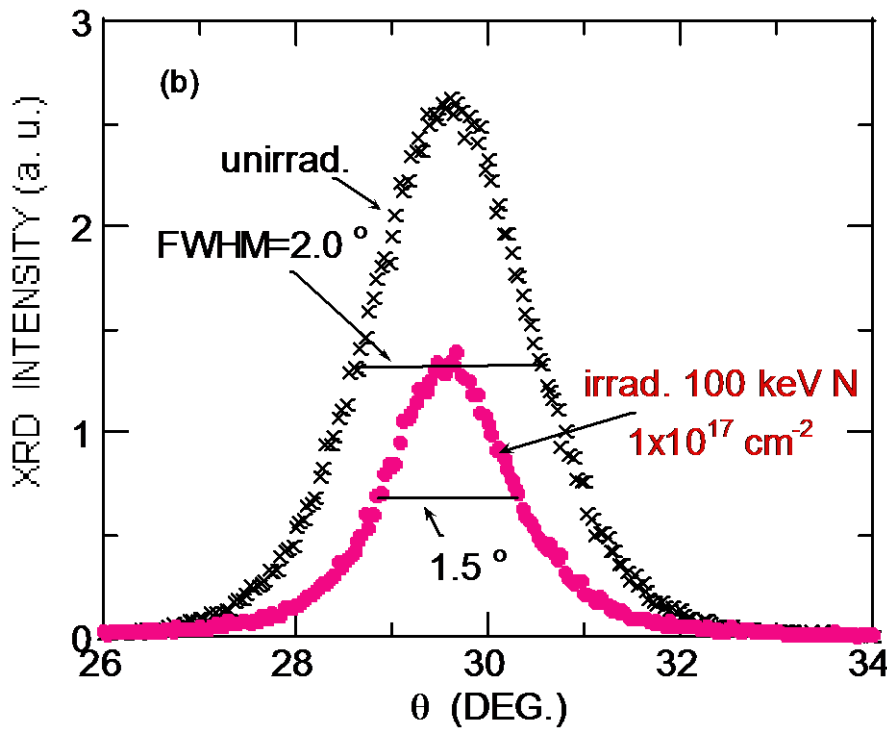
The shift of the wavelength λ_m at which the reflectivity takes their maxima & minima towards longer wavelength, with the measured refractive index => increase of film thickness

Refractive index



$\lambda_m = 4dn/j$; reflectivity minima with even integer j , maxima with odd integer j , for $n(\text{AlN}) > n(\text{Al}_2\text{O}_3) \sim 1.8$
 d : film thickness
 n : refractive index

X-ray diffraction



FWHM of XRD rocking curve decreases by N ion irradiation => alignment of grain-orientation

- Under ion irradiation,**
- Degradation of XRD intensity,
does not become amorphous
 - but **disordered state**
 - Decrease of a-axis parameter
 - No diffraction peak other than AlN & Al_2O_3

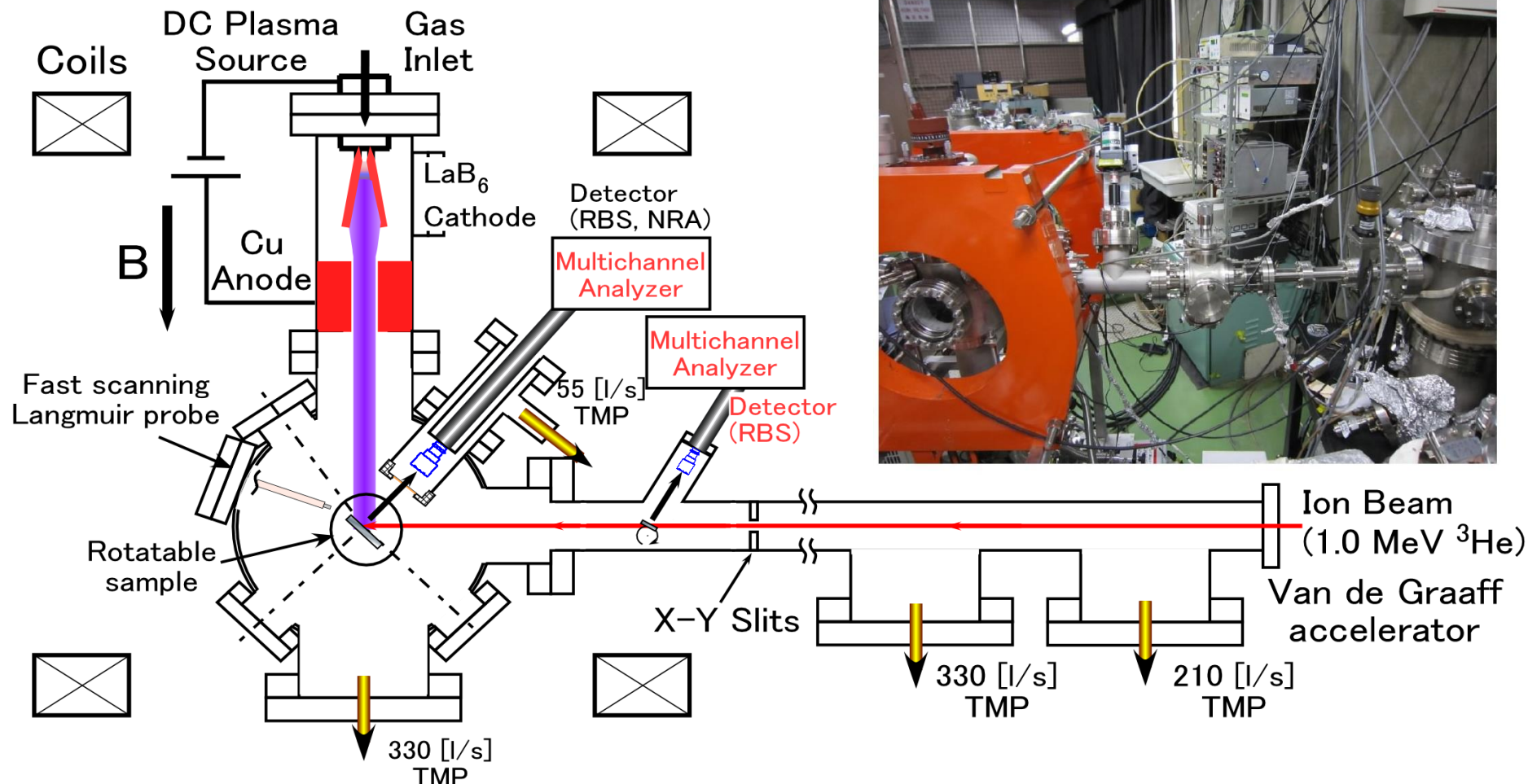
Matsunami et al, NIM
B257(2007)433.

Plasma Surface Dynamics with Ion Beam Analysis for study of dynamic retention of H isotopes under plasma exposure

PS-DIBAを用いたプラズマ照射下における水素同位体吸蔵のその場計測

Yamagiwa, Nakamura, Matsunami, Ohno, Kajita, Takagi, Tokitani,
Masuzaki, Sagara, Nishimura, Phys. Scr. T145(2011)014042.

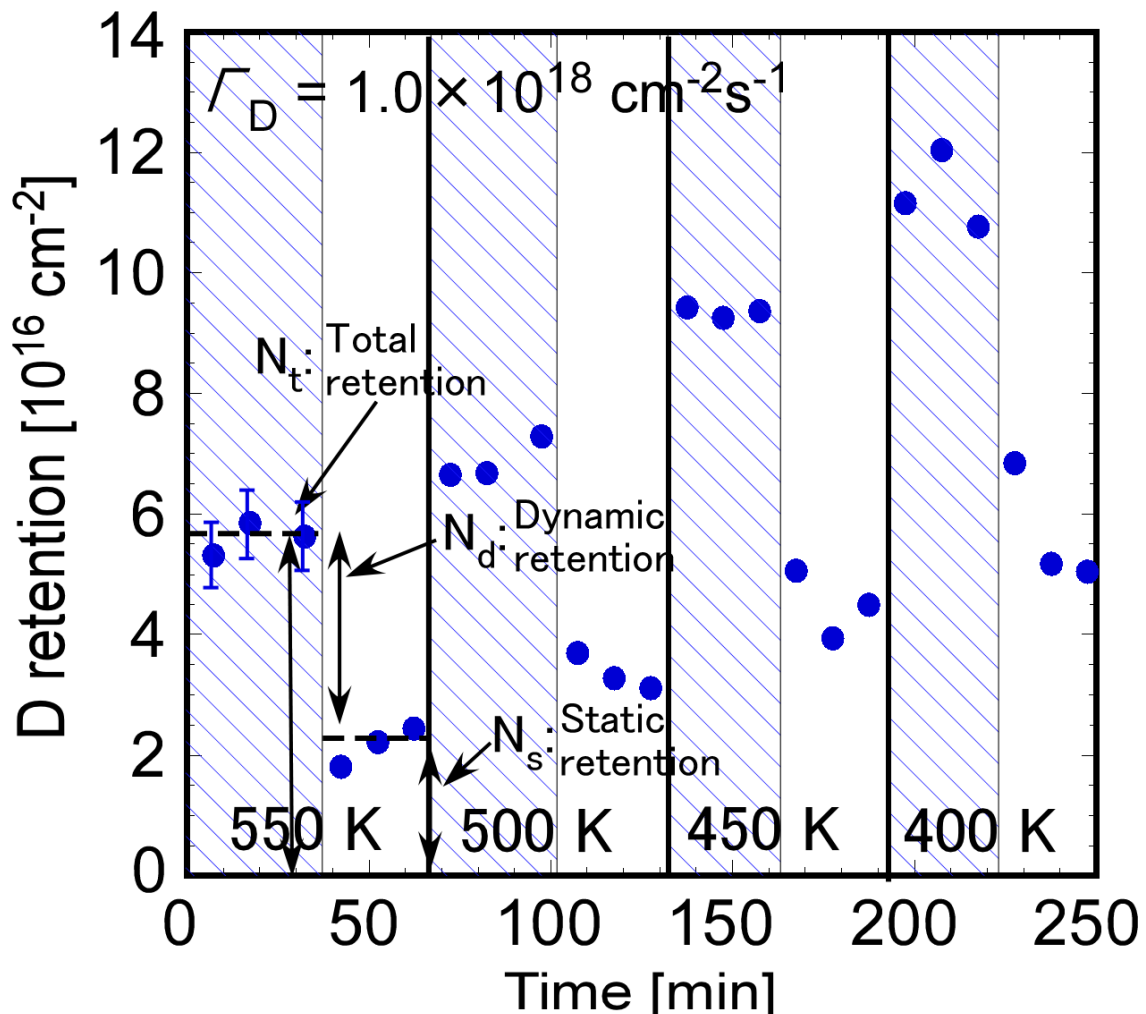
Plasma Surface Dynamics with Ion Beam Analysis (PS-DIBA)



- i) 高密度プラズマ照射下でのイオンビーム計測が可能
- ii) 差動排気によってイオンビーム検出器とVan de Graaff加速器を保護
- iii) プラズマ照射下でビーム照射量をモニタリング
- iv) 試料台の空冷によって試料温度制御

等方性黒鉛を用いた重水素吸蔵量その場計測

39



フラックス Γ_D 一定で重水素プラズマ照射
及び NRA 計測開始(斜線部)



試料温度を制御しながら、
試料への重水素イオン照射を停止



試料温度を 550K から空冷により
50K 毎に温度を下げて吸蔵量計測

プラズマ照射中

吸蔵量 $5.7 \times 10^{16} \text{ Dcm}^{-2}$
… 合計の吸蔵量 N_t

プラズマ照射停止後

吸蔵量 $1.8 \times 10^{16} \text{ Dcm}^{-2}$
… 静的吸蔵量 N_s



劇的な減少

$3.9 \times 10^{16} \text{ Dcm}^{-2}$

… 動的吸蔵量 $N_d = N_t - N_s$

ELECTRONIC SPUTTERING

40

(in collaboration with JAEA)

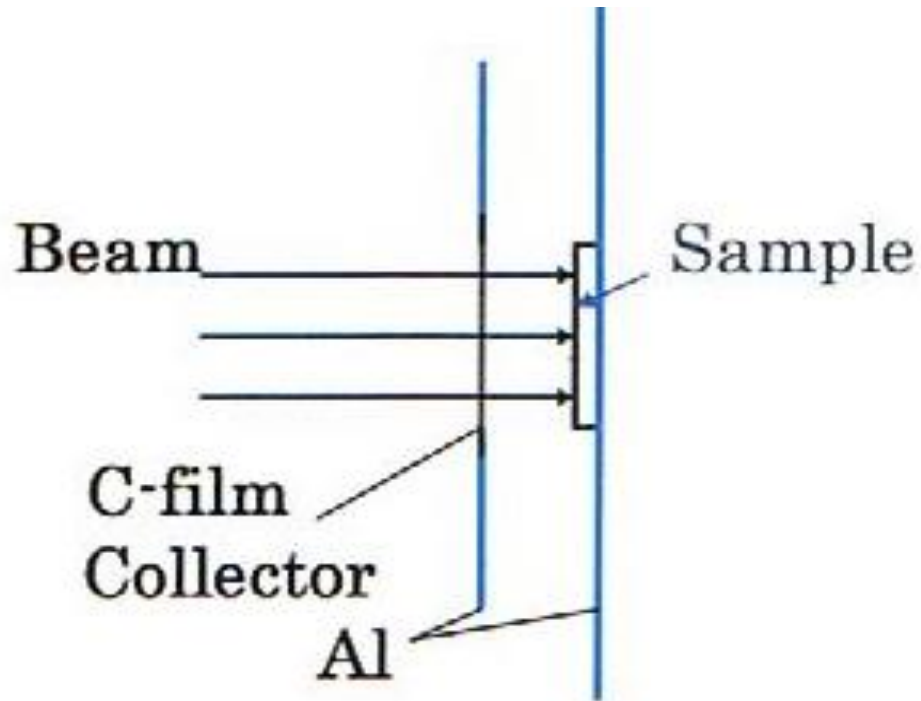
High energy ions

^{136}Xe 200, 100 MeV

^{58}Ni 90 MeV

^{40}Ar 60 MeV

(0.73 ~ 1.5 MeV/u)



Analysis of sputtered atoms: 1.8 MeV He RBS

Calibration of C-film Collection Efficiency

Samples: 15 Oxides & 3 Nitrides

a-SiO₂, c-SiO₂, ZnO, SCO, Y₂O₃, Al₂O₃, MgAl₂O₃,
MgO, SrTiO₃, TiO₂, CeO₂, Cu₂O, CuO, WO₃, ZrO₂,
Cu₃N, AlN, Si₃N₄

- Nearly stoichiometric
- From the linear relationship between sputtered atoms in Carbon-foil and ion fluence with the collector efficiency, the sputtering yields are evaluated.
- Sputtering yields Y are non linear with the electronic stopping power; $Y \propto Se^n$ with $n > 1$.

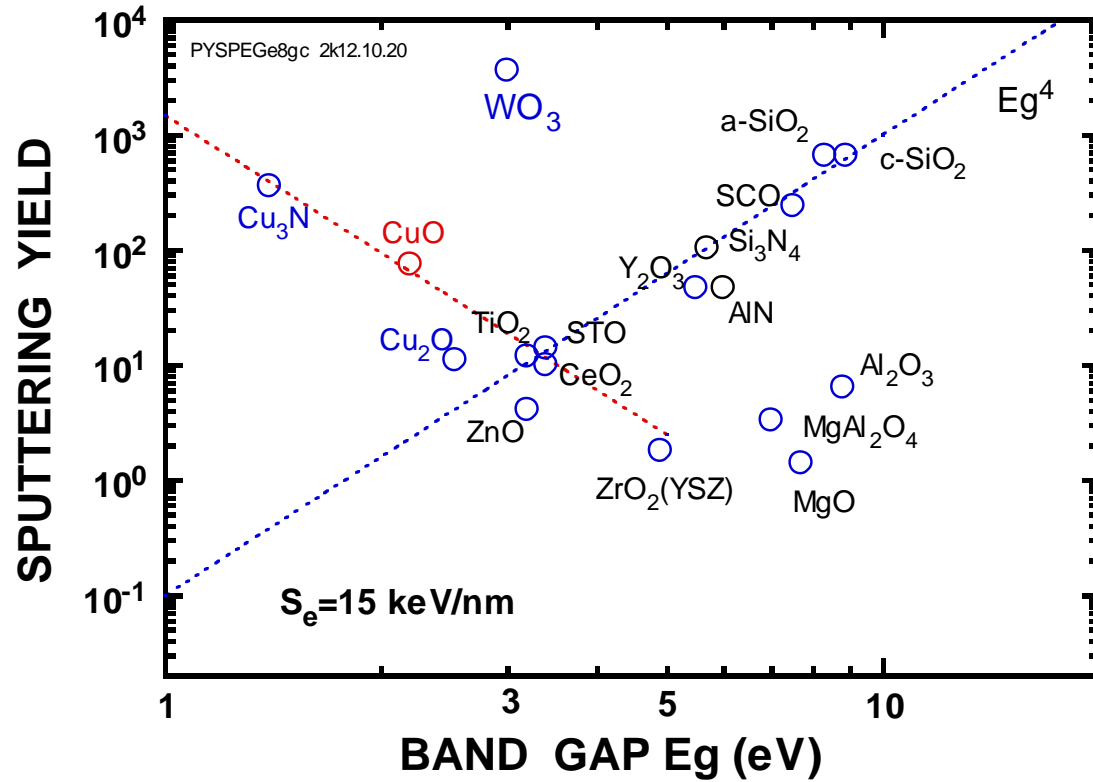
Electronic Sputtering Yield Y

(Electronic excitation effects)

**CuO, WO₃ & Cu₃N,
The erosion yields are
much larger than
the suggested
bandgap dependence.**

Electronic excitation into atomic displacement

- *Eg ~ Maximum available energy
- *Number of electron hole pairs $\propto 1/Eg$
- *Efficiency factor ?



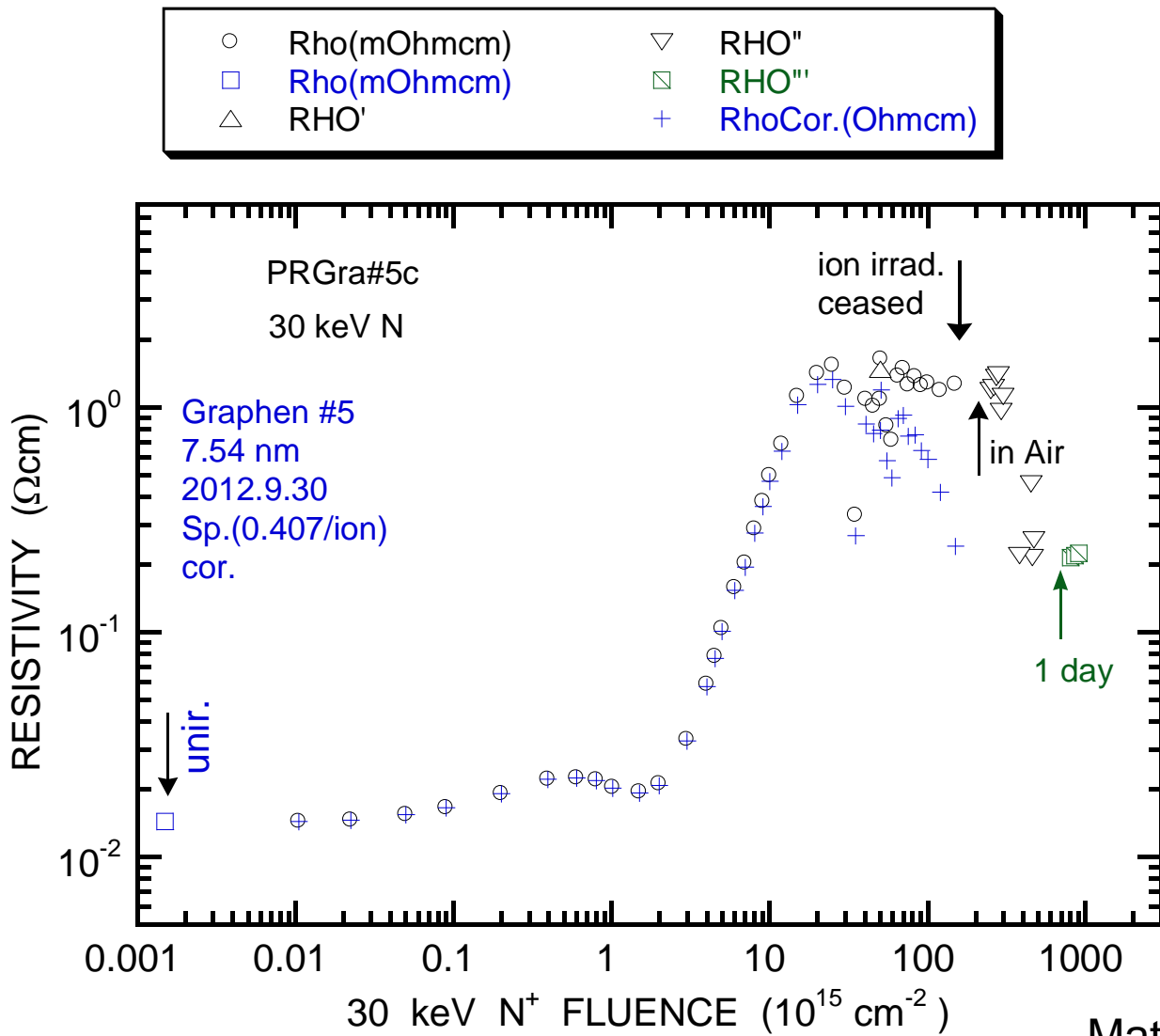
WO₃, NIM B268(2010)3167. Cu₃N, NIMB267 (2009) 2653. Cu₂O, NIM B266(2008)2986.

Mechanism of electronic sputtering?

Energy transfer from electronic system into atoms?

Ion impact effects on graphene

44

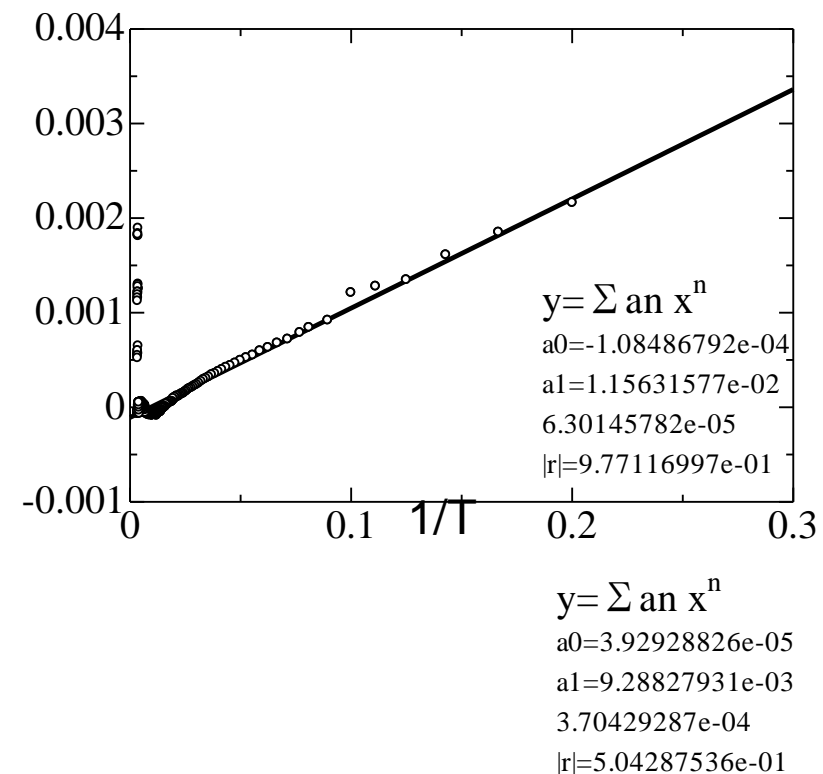
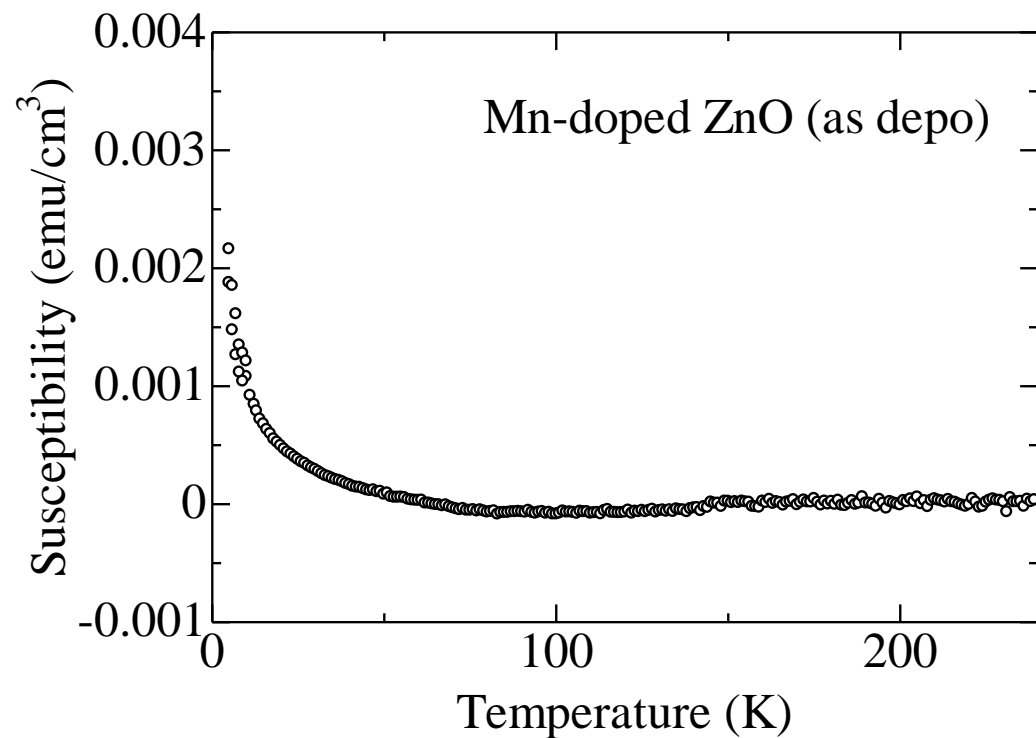


Matsunami, Tsuchiya, Mizuno,
Bandoh, 2013

magnetic property of 6%Mn-doped ZnO

Temperature dependence

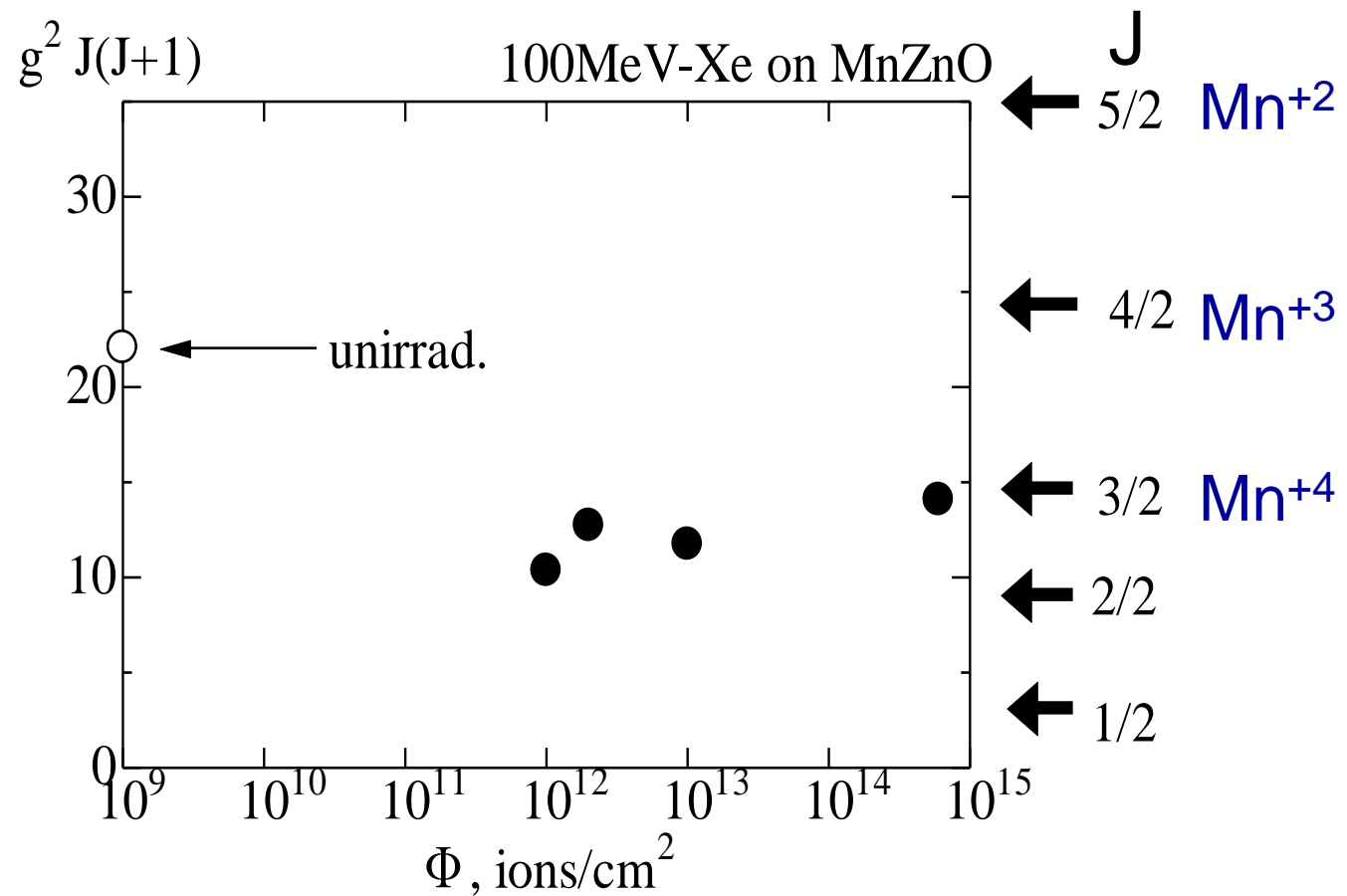
Below 150K : Curie's law \rightarrow Para-magnetic



Ion impact effect on magnetic property of 6%Mn-doped ZnO, 100 MeV Xe

46

Susceptibility
follows Curie
law (para-
magnetic)

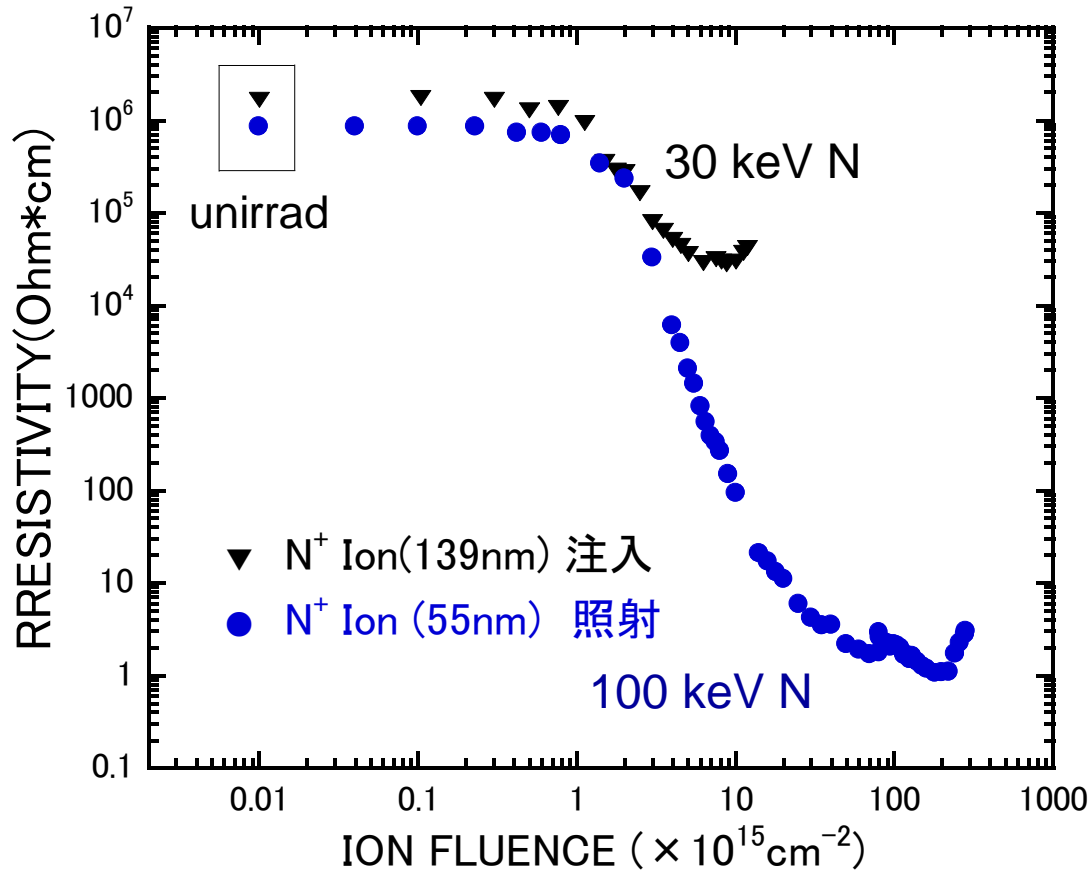


Matsunami, Okayasu, Sataka, et al. 2013

N ion energy deposition & implantation effects: Mn(6%)-doped ZnO

100 keV N
 $R_p = 160\text{nm} \gg \text{film thickness } 55\text{ nm}$
 energy deposition effect

30 keV N
 $R_p = 47\text{nm} < \text{film thickness } 140\text{ nm}$
 N ion implantation effect



Itoh, Matsunami, 2013

Concluding remarks, future problems

- Challenge
- Valency modification by ions & its effects
- Ion implantation (inclusion) effects
- Displacement threshold energy for dpa
- Mechanism of electronic excitation into atomic displacement

Thank you for your attention!